CYBERNETICS AND PHYSICS, VOL. 2, NO. 1, 2013 , 41–46

# SELF-ORGANIZED MIXED CANONICAL-DISSIPATIVE DYNAMICS FOR BROWNIAN PLANAR AGENTS

**Guillaume Sartoretti**
STI/IMT/LPM
EPFL
Switzerland
guillaume.sartoretti@epfl.ch

**Max-Olivier Hongler**
STI/IMT/LPM
EPFL
Switzerland
max.hongler@epfl.ch

**Abstract**

We consider a collection of $N$ homogeneous interacting Brownian agents evolving on the plane. The time continuous individual dynamics are jointly driven by mixed canonical-dissipative (MCD) type dynamics and White Gaussian noise sources. Each agent is permanently at the center of a finite size observation disk $D_\rho$. Steadily with time, agents count the number of their fellows located in $D_\rho$. This information is then used to re-actualize control parameters entering into the MCD. Dissipation mechanisms together with the noise sources ultimately drive the dynamics towards a consensual stationary regime characterized by an invariant measure $P_s$ on an appropriate probability space. Assuming propagation of chaos, a mean field approach enables to analytically calculate $P_s$. For each agent, our dynamics naturally implement: i) a trend to not be isolated, ii) a trend to avoid strong promiscuity, and iii) an overall trend to be attracted to a polar point. The MCD drift is derived from a Hamiltonian function $\mathcal{H}$ and incites the agents to follow one consensual orbit coinciding with a level curve of $\mathcal{H}$. When $\mathcal{H}$ is the harmonic oscillator, we are able to analytically derive the consensual orbit as a function of the size of $D_\rho$. Generalizations involving more complex $\mathcal{H}$ are explicitly worked out. Among these illustrations, we study a Hamiltonian whose level curves are the Cassini's ovals. A selection of simulations experiments corroborating the theoretical findings are presented.

**Key words**

Homogeneous Brownian agents, limited-range mutual interactions, consensual orbit generation, mixed canonical-dissipative dynamics, mean-field description, analytical results.

## 1 Introduction

The emergence of structured collective dynamical patterns from simple agent level behaviors as observed in nature for fishes, birds, insects and the like inspires a sustained research activity in management and control of complex systems, and particularly in the domain of swarm robotics. The capability of agents to act asynchronously to determine specific trajectories by relying only on local sensing is definitely attractive when a centralized control becomes unfeasible - for example to coordinate large assemblies of autonomous robots or other agents. One possibility to address these difficult global control issues is by implementing dynamic strategies where identical robots are programmed with elementary features requiring limited on-board real time sensing and computational resources. This general and truly simple idea triggers a strong interdisciplinary research activity which, as emphasized in the recent review (Gazi and Fidan, 2007), encompasses a relatively wide spectrum of perspectives ranging from ethology to swarm robotics. Focusing here on the dynamic system and control perspectives, we study a collection of asynchronously interacting point Brownian agents obeying elementary coordination algorithms. The basic ingredients of our modeling are: i) a Hamiltonian function $\mathcal{H}$ which provides a parametric family of non-intersecting level curves defining closed orbits, ii) a mixed conservative and gradient vector field constructed from $\mathcal{H}$ involving one (or several) control parameters, iii) a stochastic driving stylized by WGN's sources and iv) for each agent, a circular observation range $D_\rho$ with radius $\rho$, centered at each agent location. The agents mutual interactions directly depend on the size of $D_\rho$. Interactions produce an adaptive mechanism which drives the agents to ultimately adopt one (or several) consensual value(s) of the control parameter(s). The emerging consensual parameter(s) value selects one specific orbit among the Hamiltonian parametric family. For such mixed canonical-dissipative stochastic dynamics, connected with models discussed in (Hongler and Ryter, 1978), we are able to explicitly write the resulting invariant probability measure solving the associ-

ated time-independent non-linear *Fokker-Planck* equation (NLFP). We can therefore analytically investigate the influence of the radius $\rho$ of the observation range $D_\rho$ on the emerging consensual dynamics achieved by the agents. While our class of dynamics presents similarities with potential-ruled algorithms as those used for example in (Gazi and Passino, 2004; Gazi and Fidan, 2007; Hsieh, Kumar and Chaimowicz, 2008; Sepulchre, Paley and Leonard, 2008), it however keeps a decentralized mechanism stylized in the basic agents models pioneered by (Reynolds, 1987; Vicsek, Czirk, Ben-Jacob, Cohen and Shochet, 1995) and more recently by (Cucker and Smale, 2007).

Mathematically speaking, our modeling relies on a set of $N$ continuous time, coupled nonlinear stochastic differential equations (SDE) driven by White Gaussian noise (WGN). In this context, the basic formal question, first raised first by H. McKean (McKean Jr., 1966), is to calculate the limit of the probability distribution which describes a large agent collection (i.e. formally the thermodynamic limit $N \to \infty$) and then fluctuations around this limit for finite $N$. Considering that all agents have random identical independent initial conditions, one mathematically expects (this can be rigorously proved under somehow restricting technical hypothesis) that in the thermodynamic limit, all finite number of agents behaves independently of the others and they can all be described by the same probability distribution (this is known as *propagation of chaos*). The common probability distribution solves a Markovian evolution described by a nonlinear Chapman-Kolmogorov type partial differential equation. Accordingly, when propagation of chaos holds, we may characterize the dynamic behavior of the global population by only studying the dynamics of a single, randomly chosen, agent subject to an effective external *mean-field* generated by its surrounding fellows. In presence of WGN's sources, the single representative agent follows a diffusion process and its probability measure obeys to a NLFP, (Frank, 2005).

## 2 Interacting Brownian Agents Driven by Canonical-Dissipative Dynamics and White Gaussian Noise

We consider a swarm of $N$ mutually interacting dynamical agents $a_k$ for $k = 1, 2, \cdots, N$ evolving on the plane $\mathbb{R}^2$ with state variables $\vec{X}(t) = (X_1(t), X_2(t), \cdots, X_N(t))$. In this section, we assume the homogeneous situation in which all individual isolated agents $a_k$ are dynamically identical. The collective dynamics is assumed to obey an $N$-dimensional diffusion process on $\mathbb{R}^2$ given by a set of stochastic differential equations (SDE):

$$\begin{cases} d\mathbf{X}_k(t) = \mathbb{A}_k(t)\mathbf{X}_k(t)\,dt + \overbrace{\gamma\left[\mathcal{L}^2_{k,\rho}(t) - \|\mathbf{X}_k(t)\|_2^2\right]\mathbf{X}_k(t)}^{\mathcal{C}_k(\mathbf{X}_k(t))} \\ \qquad\qquad dt + \sigma\, d\mathbf{W}_k(t), \qquad k = 1, 2, \cdots, N, \\ \mathbf{X}_k(0) = \mathbf{X}_{0,k}, \qquad \text{and} \qquad \mathbf{X}_k(t) \in \mathbb{R}^2. \end{cases} \tag{1}$$

In Eq.(1), the following notations are used: $\mathbf{X}_k(t) = (x_{k,1}(t), x_{k,2}(t)) \in \mathbb{R}^2$, the usual norm $\|\mathbf{X}_k(t)\|_2^2 := \left(x^2_{k,1}(t) + x^2_{k,2}(t)\right)$, $\gamma$ and $\sigma$ are positive constants common to all $a_k$ (i.e. homogeneity assumption) and $\mathbf{W}_k(t) = (W_{k,1}, W_{k,2})_{t\geq 0}$ are independent standard Brownian Motions (BM) and hence the formal differentials $dW_k(t)$ are White Gaussian Noise (WGN) processes. The agents interactions will be defined via the scalars $\mathcal{L}^2_{k,\rho}(t)$ and the matrices $\mathbb{A}_k(t)$ which both will depend on $\mathcal{D}_{k,\rho}(t)$ the set of instantaneous neighboring fellows surrounding agent $a_k$ at time $t$. For a given observation range $\rho$, the $a_k$-*instantaneous observation neighborhood* $\mathcal{D}_{k,\rho}(t)$ is the disk:

$$\mathcal{D}_{k,\rho}(t) = \left\{\mathbf{X} \in \mathbb{R}^2 \mid \|\mathbf{X} - \mathbf{X}_k(t)\|_2 \leq \rho\right\} \tag{2}$$

and we define the indices set

$$V_{k,\rho}(t) = \left\{i \mid \mathbf{X}_i(t) \in \mathcal{D}_{k,\rho}(t)\right\}. \tag{3}$$

which identifies the $a_k$-neighboring agents present in the disk $\mathcal{D}_{k,\rho}(t)$. We shall write $N_{k,\rho}(t) := |V_{k,\rho}(t)|$ the cardinality of the set $V_{k,\rho}(t)$. The dynamic elements contained in Eq.(2) and Eq.(3) are now used to characterize the agents' mutual interactions via a couple of contributions:

i) **Canonical-dissipative matrix** $\mathbb{A}_k(t)$. The dynamic matrix $\mathbb{A}_k(t)$ associated with agent $a_k$ can be defined as:

$$\mathbb{A}_k(t) := \begin{pmatrix} \frac{N_{k,\rho}(t)}{N} - \frac{1}{M} & \frac{N_{k,\rho}(t)}{N} \\ -\frac{N_{k,\rho}(t)}{N} & \frac{N_{k,\rho}(t)}{N} - \frac{1}{M} \end{pmatrix}, \tag{4}$$

with $1 \leq M \leq N$ and $N_{k,\rho}(t)/N$ is the fraction of the total swarm that agent $a_k$ detects in $\mathcal{D}_{k,\rho}(t)$ (we shall adopt the convention that agent $a_k$ systematically detects itself, implying that $N_{k,\rho}(t) \geq 1$, $\forall\, t$). As $\mathbf{X}_k = 0$ is a singular point of the deterministic dynamics (i.e. obtained for $\sigma = 0$ in Eq.(1)) the matrix $\mathbb{A}_k(t)$ formally stands for the linear mapping of the dynamics in the neighbourhood of the origin. The associated couple of eigenvalues of $\mathbb{A}_k(t)$ read:

$$\lambda_{k,\pm}(t) = \underbrace{\left[\frac{N_{k,\rho}(t)}{N} - \frac{1}{M}\right]}_{:=\mathcal{R}_{k,\rho}(t)} \pm (\sqrt{-1}) \underbrace{\left[\frac{N_{k,\rho}(t)}{N}\right]}_{:=\mathcal{I}_{k,\rho}(t)}. \tag{5}$$

Hence, at a given time $t$, the real part in Eq.(5) expresses the non-conservative type of the dynamics (i.e. the divergence part of the vector field (VF)).

The singular point $\mathbf{0} \in \mathbb{R}^2$ is an attractive (respectively repulsive) node when $\mathcal{R}_{k,\rho}(t) < 0$ (resp. $\mathcal{R}_{k,\rho}(t) > 0$). Moreover, the component $\mathcal{I}_{k,\rho}(t)$ expresses the rotational nature of the VF. In particular, when $\mathcal{R}_{k,\rho}(t) = 0$, the dynamics are conservative; it expresses the *Hamiltonian* component of the $a_k$-VF.

ii) **Adaptive limit cycle radius**. The scalar quantity

$$\mathcal{L}^2_{k,\rho}(t) := \frac{1}{|V_{k,\rho}(t)|} \sum_{j \in V_{k,\rho}(t)} \|X_j(t)\|_2^2 \qquad (6)$$

defines the (square) of the radial position of the barycenter of the agents belonging to $\mathcal{D}_{k,\rho}$.

**Proposition 1**. *Consider the* **mixed-canonical dissipative diffusive dynamics** *Eq.(1). Asymptotically with times, the dynamics propagates chaos and the MF representative agent obeys to the couple of diffusion equations :*

$$\begin{cases} dX_1(t) = +\frac{1}{M} X_2(t) + \gamma \left[\mathcal{L}^2_{s,\rho} - (X_1^2(t) + X_2^2(t))\right] \\ \qquad\qquad \cdot X_1(t)\, dt + \sigma dW_1(t), \\ dX_2(t) = -\frac{1}{M} X_1(t) + \gamma \left[\mathcal{L}^2_{s,\rho} - (X_1^2(t) + X_2^2(t))\right] \\ \qquad\qquad X_2(t)\, dt + \sigma dW_2(t). \end{cases} \qquad (7)$$

*For weak noise (i.e. large values of $\gamma/\sigma^2$), the radius approximately reads $\mathcal{L}_{s,\rho} \simeq \frac{\rho}{\sqrt{2(1-\cos(\pi/M))}}$ and the associated stationary probability density $P_s(\mathbf{x})$ reads:*

$$P_s(\mathbf{x}) dx_1 dx_2 = \frac{\exp\left\{\frac{2\gamma}{\sigma^2}\left[\mathcal{L}^2_{s,\rho} - (x_1^2 + x_2^2)\right]\right\} dx_1 dx_2}{\mathcal{Z}}, \qquad (8)$$

*with $\mathbf{x} = (x_1, x_2) \in \mathbb{R}^2$, and $\mathcal{Z}$ being the probability normalization factor.*

**Proof of Proposition 1**.

The Fokker-Planck equation associated with the diffusion process of Eq.(1) can be written in the form:

$$\partial_t P(\vec{\mathbf{x}}, t|\vec{\mathbf{x_0}}) = -\bigtriangledown \cdot \Big\{ \tfrac{1}{2}\left[\mathbb{A}_a(t) \bigtriangledown \|\vec{\mathbf{x}}\|^2 - \bigtriangledown V_\rho\,(t, \vec{\mathbf{x}})\right] P(\vec{\mathbf{x}}, t|\vec{\mathbf{x_0}}) + \tfrac{\sigma^2}{2} \bigtriangledown P(\vec{\mathbf{x}}, t|\vec{\mathbf{x_0}}) \Big\}, \qquad (9)$$

where $\mathbb{A}_a$ is the $(2N \times 2N)$ block-simplectic matrix:

$$\mathbb{A}_a(t) := \begin{pmatrix} B_1(t) & & 0 \\ & \ddots & \\ 0 & & B_N(t) \end{pmatrix},$$

$$\text{with } B_k(t) = \begin{pmatrix} 0 & \frac{N_{k,\rho}(t)}{N} \\ -\frac{N_{k,\rho}(t)}{N} & 0 \end{pmatrix}$$

and the *time-dependent* generalized potential $V_\rho\,(t, \vec{\mathbf{x}})$ from which the dissipative component of the drift is derived, can be written as:

$$V_\rho\,(t, \vec{\mathbf{x}}) = \sum_{k=1}^N \Bigg\{ \overbrace{\tfrac{1}{2}\left[\frac{N_{k,\rho}(t)}{N} - \frac{1}{M}\right]}^{:=\mathcal{R}_{k,\rho}(t)} \|\vec{\mathbf{x}}\|^2 + \tfrac{\gamma}{2}\left[\mathcal{L}^2_{k,\rho}(t) - \|\vec{\mathbf{x}}\|^2\right]^2 \Bigg\}. \qquad (10)$$

The potential parameterization $\mathcal{R}_{k,\rho}(t)$ and $\mathcal{L}^2_{k,\rho}(t)$ in Eq.(10) explicitly depends on the agents' configurations implying that Eq.(9) is effectively a NLFP. The potential $V_\rho\,(t, \vec{\mathbf{x}})$ is globally attractive on $\mathbb{R}^{2N}$, (i.e $V_\rho\,(t, \vec{\mathbf{x}}) \to \infty$ for $\|\vec{\mathbf{x}}\| \to \infty$). Global attraction together with the WGN driving sources imply that the diffusive dynamic Eq.(1) is *ergodic* on $\mathbb{R}^{2N}$. Accordingly, it exists a unique invariant measure $P_s(\vec{\mathbf{x}})$ and therefore both $\mathcal{R}_{k,\rho}(t)$ and $\mathcal{L}^2_{k,\rho}(t)$ asymptotically converge to stationary (i.e time-independent) values $\mathcal{L}^2_{k,s,\rho}$ and $\mathcal{R}_{k,s,\rho}$. Eqs.(9) and (10) being explicitly invariant under permutations in the agents labeling, we shall also have $\mathcal{L}^2_{k,s,\rho} = \mathcal{L}^2_{s,\rho}$ and $\mathcal{R}_{k,s,\rho} = \mathcal{R}_{s,\rho}$. Finally, in the stationary regime, the system is driven to its minimal energy configuration implying here that $\mathcal{R}_{s,\rho} \equiv 0$. This in turn yields that $\lim_{t\to\infty} \mathbb{A}_a(t) = \mathbb{A}_{a,s}$ with:

$$\mathbb{A}_{a,s} := \begin{pmatrix} \mathbb{A}_s & & 0 \\ & \ddots & \\ 0 & & \mathbb{A}_s \end{pmatrix}, \qquad \mathbb{A}_s = \begin{pmatrix} 0 & \frac{1}{M} \\ -\frac{1}{M} & 0 \end{pmatrix}.$$

The gradient $\bigtriangledown V_\rho\,(t, \vec{\mathbf{x}})$ is systematically orthogonal to the antisymmetric component $\frac{1}{2}\mathbb{A}_a(t) \bigtriangledown \|\mathbf{x}\|^2$ (this remains true for the stationary regime $A_{a,s}$). It enables to write the stationary solution of Fokker-Planck Eq.(9) in the *product-form* $P_s(\vec{\mathbf{x}})$:

$$\begin{aligned} P_s(\vec{\mathbf{x}}) &= [P_s(\mathbf{x})]^N = \left[\mathcal{N}^{-1} e^{\{V_{s,\rho}(\mathbf{x})\}}\right]^N, \\ V_{s,\rho}(\mathbf{x}) &= +\tfrac{\gamma}{2}\left[\mathcal{L}^2_{s,\rho} - \|\mathbf{x}\|^2\right]^2 \end{aligned} \qquad (11)$$

with the notation $\vec{\mathbf{x}} = (\mathbf{x}_1, \mathbf{x}_2, \cdots, \mathbf{x}_N) \in \mathbb{R}^{2N}$, $\mathbf{x}_k \in \mathbb{R}^2$ and $\mathbf{x} \in \mathbb{R}^2$ stands for one representative agents among the collection of the $\mathbf{x}_k$'s. The product form of the invariant measure explicitly shows that our dynamics propagates chaos, validating the use of a MF approach where a single agent behavior effectively reflects the global dynamics.

Taking the MF approach, and focusing on the stationary regime, from the point of view of a single representative planar agent $\mathbf{X}(t) = (x_1(t), x_2(t))$, we have:

$$0 = \bigtriangledown\Big\{ \tfrac{1}{2}\left[\mathbb{A}_s \bigtriangledown \|\mathbf{x}\|^2 - \bigtriangledown V_{s,\rho}\,(\mathbf{x})\right] \cdot P_s(\mathbf{x})\Big\} - \tfrac{\sigma^2}{2} \triangle P_s(\mathbf{x}), \qquad (12)$$

where $P_s(\mathbf{x})$ is the invariant probability density.

Within the stationary regime, autoconsistency implies

$$\frac{N_{s,\rho}}{N} = \int_{(\mathbf{x}) \in D_\rho} P_s(\mathbf{x})\, dx_1\, dx_2 \left(= \frac{1}{M}\right) \qquad (13)$$

and

$$\mathcal{L}^2_{s,\rho} = \int_{(x_1,x_2)\in D_\rho} \left(x_1^2 + x_2^2\right) P_s(\mathbf{x})\, dx_1\, dx_2, \qquad (14)$$

where $D_\rho$ is the representative agent's neighborhood.

From a uniformly rotating coordinates' frame with angular velocity $M^{-1}$, the stationary regime dynamics becomes purely gradient and the resulting probability density $P_s(\mathbf{x})$ solving Eq.(12) enjoys microscopic reversibility (i.e. *detailed balance*). It explicitly reads, (Hongler and Ryter, 1978):

$$\begin{aligned} &P_s(\mathbf{x}) dx_1 dx_2 = P_s(r) dr\, d\theta = \\ &= \mathcal{N}(\mathcal{L}_{s,\rho})\, e^{\left[-\frac{\gamma}{\sigma^2}(r^2 - \mathcal{L}^2_{s,\rho})^2\right]} d(r^2)\, d\theta. \end{aligned} \qquad (15)$$

with $\mathcal{N}^{-1}(\mathcal{L}_{s,\rho}) = \sqrt{\pi^3\sigma^2/\gamma}\,\mathrm{Erfc}\left(-\frac{\sqrt{\gamma}\,(\mathcal{L}^2_{s,\rho})}{\sigma}\right)$ being the normalization factor.

In this stationary regime, the stationary observation neighborhood of each agent exactly encompasses a circular sector with aperture $\varphi(M)$ and radius $\mathcal{L}^2_{s,\rho}(M)$. Both $\varphi(M)$ and $\mathcal{L}_{s,\rho}(M)$ are adjusted to ensure that $N/M$ agents are located in $\mathcal{D}_{s,\rho}$. For large ratio $\frac{\gamma}{\sigma^2}$ (i.e. essentially a large signal-to-noise ratio), Eq.(15) exhibits a sharply peaked "mexican hat" shape with its maximum on the circle $r = \mathcal{L}_{s,\rho}$ (i.e. almost all agents stay confined in the direct neighborhood of the circle $r = \mathcal{L}_{s,\rho}$).

As detailed in Figure 1's caption, an elementary trigonometric argument enables to derive the compact relation:

$$\mathcal{L}_{s,\rho} = \frac{\rho}{\sqrt{2 - 2\cos(\pi/M)}}. \qquad (16)$$

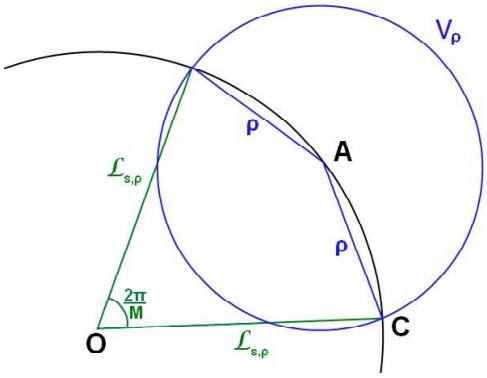


Figure 1: The cylindrical symmetry characterizing the stationary regime implies that the agents probability distribution is rotationally invariant with respect to **O**. Accordingly, there will be on average $N/M$ agents located in a sector with an opening angle $2\pi/M$. For large $\gamma/\sigma^2$, these agents will be confined in the direct proximity of the circle of radius $\mathcal{L}_{s,\rho}$. Let us consider an arbitrary agent located at **A** with a stationary observation range of radius $\rho = \mathbf{AC}$. This range exactly encompasses the circular arc with aperture $2\pi/M$ thus ensuring that the agent at **A** has $M/N$ neighboring fellows. The cosine theorem in the triangle **OAC** implies that $\mathcal{L}^2_{s,\rho} = 2\rho^2/\left[1-\cos(\pi/M)\right] 2\mathcal{L}^2_{s,\rho} = \rho^2/\left[1-\cos(\pi/M)\right]$. □

**Additional remarks**. Observe that besides $\gamma$ and $\sigma$ which define an overall time scale, there are two additional control parameters in the dynamics Eq.(1):

a) **Hamiltonian parameter** $M$. The sector angle $M$ into the canonical-dissipative matrix $\mathbb{A}(t)$. This parameter fixes the angular velocity $\omega = M^{-1}$ of the swarm and adjusts the size of the consensual limit cycle radius $\mathcal{L}_{s,\rho}$. For a given size of the observation disk with radius $\rho$ and for large $M$, we have $\mathcal{L}_{s,\rho} \simeq \rho M/\pi$ and the angular velocity tends to vanish.

b) **Interaction range parameter** $\rho$. The radius of the observation disk $\rho$ which directly determines the consensual size of the limit cycle radius $\mathcal{L}_{s,\rho}$.

## 3 Numerical Experiments

In all numerical experiments performed, we observe a truly remarkable agreement with the theoretical predictions (see Figure 2 for a specific illustration). According to Eq.(16), by reducing the sector opening angle (i.e by increasing the values of the $M$), the resulting limit cycle radius $\mathcal{L}_{s,\rho}$ increases and the number of agents present in $\mathcal{D}_{s,\rho}$ is reduced thus somehow invalidating the large population required for MF to be used. Even when $M = 50$, the couple of orbits realizations shown in Figure 3 show that analytical results, in particular Eq. (16), remain valid in this large $M$ limit.

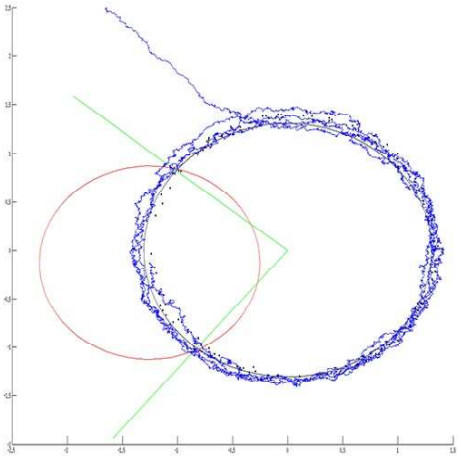

Figure 2: For a collection of $N = 100$ agents with $M = 4$ and $\rho = 1$. The observation range of the considered agent encompasses exactly the sector of aperture $\pi/4$ to determine the size of the self-generated limit cycle (see the construction given in Figure 1). We explicitly draw the trajectory of a randomly chosen agent and observe that this agent indeed follows the consensual limit cycling orbit with analytically predicted radius $\mathcal{L}_{s,\rho} = \sqrt{2}\rho = \sqrt{2}$.

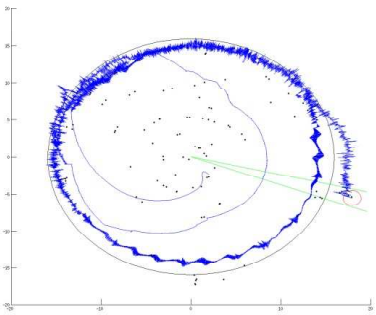

Figure 3: For a collection of $N = 100$ agents with $M = 50$ and $\rho = 1$. The observation range of the considered agent encompasses exactly the narrow sector of aperture $\pi/50$ to determine the size of the self-generated limit cycle (see the construction given in Figure 1). We explicitly draw the trajectory of a randomly chosen agent and observe that this agent indeed follows the consensual limit cycling orbit with analytically predicted radius $\mathcal{L}^2_{s,\rho} = 2/\left[1-\cos(\pi/50)\right] \simeq (50/\pi)^2 \simeq (17)^2$. The High value $M = 50$ is responsible for the sometimes erratic behaviour of the agent, as its observation range only encompasses a very small sector of the consensual circle.

## 4 Generalization

By using the class of mixed-canonical dissipative dynamics (Hongler and Ryter, 1978) and following the same lines as those given in Proposition 1, we now can relax the cylindrical symmetry and write:

**Proposition 2**. *Consider the class of functions* $\mathcal{H}(x_1, x_2) : \mathbb{R}^2 \mapsto \mathbb{R}^+$ *for which the family of planar curves defined by* $[\mathcal{H}(x_1, x_2) - R] = 0$ *are closed* $\forall\ R > 0$ *and do not intersect for different values of* $R$*'s. Introduce the functional* $\mathcal{V}(\mathcal{H}) : \mathbb{R}^+ \mapsto \mathbb{R}$ *with* $\lim_{\mathcal{H}\to\infty} \mathcal{V}(\mathcal{H}) = \infty$*. Assume in addition that the values of the* $\mathcal{H}$*-derivatives* $\mathcal{V}'(0) < 0$ *and* $\mathcal{V}'(\mathcal{H}) \mid_{\mathcal{H}=C} = 0$ *and* $C$ *is the unique value for which it holds. Then Eqs.(1) and (7) can be respectively generalized as:*

$$\begin{cases} d\mathbf{X}_k(t) = \mathbb{A}_k(\vec{\mathbf{X}})\, dt - \gamma \left\{ \mathcal{V}'(\mathcal{H}(\mathbf{X})) \partial_{\mathbf{X}_k} \mathcal{H}(\mathbf{X}_k) \right\} dt \\ \qquad\qquad +\sigma\, d\mathbf{W}_k(t), \qquad k = 1, 2, \cdots, N, \\ \\ X_k(0) = X_{0,k}, \qquad \text{and} \qquad X_k(t) \in \mathbb{R}^2, \end{cases} \tag{17}$$

where

$$\mathbb{A}_k(\vec{\mathbf{X}}) = \begin{pmatrix} \frac{N_k(t)}{N} - \frac{1}{M} & \frac{N_k(t)}{N} \\ \\ -\frac{N_k(t)}{N} & \frac{N_k(t)}{N} - \frac{1}{M} \end{pmatrix} \cdot \begin{pmatrix} \partial_{X_{1,k}} \mathcal{H}(\mathbf{X}_k) \\ \\ \partial_{X_{2.k}} \mathcal{H}(\mathbf{X}_k) \end{pmatrix} \tag{18}$$

and

$$\begin{cases} dX_1(t) = \big[ + \frac{1}{M} \partial_{X_2} \mathcal{H}(\mathbf{X}) - \gamma \big\{ [\mathcal{V}'(\mathcal{H}(\mathbf{X})] \\ \qquad\qquad \cdot \partial_{X_1} \mathcal{H}(\mathbf{X}) \big\} \big] dt + \sigma dW_1(t), \\ \\ dX_2(t) = \big[ - \frac{1}{M} \partial_{X_1} \mathcal{H}(\mathbf{X}) - \gamma \big\{ [\mathcal{V}'(\mathcal{H}(\mathbf{X})] \\ \qquad\qquad \cdot \partial_{X_2} \mathcal{H}(\mathbf{X}) \big\} \big] dt + \sigma dW_2(t). \end{cases} \tag{19}$$

*The stationary measure Eq.(8) here reads:*

$$P_s(\mathcal{H})\, d\mathcal{H} = \mathcal{Z}^{-1} \exp\left\{ \frac{2\gamma}{\sigma^2} [\mathcal{V}(\mathcal{H})] \right\} d\mathcal{H}, \tag{20}$$

*where* $\mathcal{Z}$ *is the normalization constant.*

□

**Additional remarks**.

a) Observe that Proposition 1 follows from the Proposition 2 in the rotationally symmetric case resulting when $\mathcal{H}(\mathbf{X}) = (1/2) \left[ X_1^2 + X_2^2 \right]$.
b) Contrary to Proposition 1, in Proposition 2, neither the limit cycle nor the invariant measure $P_s(\mathcal{H})$ generally have a cylindrical symmetry. This precludes the possibility to analytically determine the selected consensual limit cycle (i.e we do not have in the general case a simple expression like the one given by Eq.(16)).
c) As an illustration of Proposition 2, we may consider the Cassini Hamitonian function given by

$$\mathcal{H}(\mathbf{X}) = \left[ (x_1 - 1)^2 + x_2^2 \right] \left[ (x_1 + 1)^2 + x_2^2 \right] = b^4, \tag{21}$$

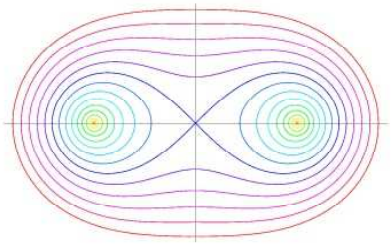

Figure 4: Typical shapes of the Cassini's ovals determined by the equation $\mathcal{H}(x_1, x_2) = \left[ (x_1 - 1)^2 + x_2^2 \right] \left[ (x_1 + 1)^2 + x_2^2 \right] = b^4$ for $b$-values ranging from $b = 0.1$ to $1.5$.

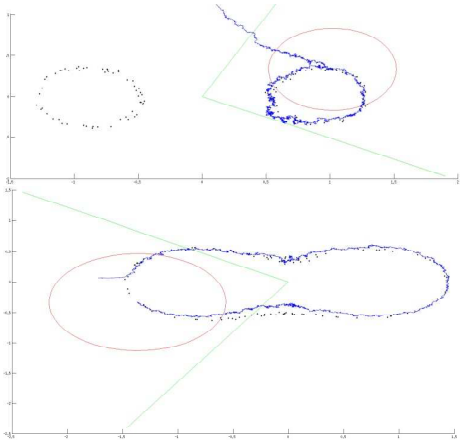

Figure 5: Top: Selection of a couple of limit cycling orbits obtained from the Cassini Hamiltonian Eq.(21) when the control parameters are set to $M = 4$ and $\rho = 0.4$.
Bottom: Single limit cycling trajectory for the Cassini Hamiltonian Eq.(21) but here with the control parameters set to $M = 4$ and $\rho = 0.8$.

with the level orbits sketched in Figure 4. According to the values of $M$ and $\rho$ which ultimately will fix the size of the parameter $b$, we are in this case able to generate two different regimes. For large $b$ a single closed consensual limit cycle is generated. Alternatively, for small $b$, the agents are shared into two clusters and evolve on two separated consensual limit cycles (see Figure 5).
d) Generalizing the previous Cassini ovals construction, one may construct Hamiltonian generating agents circulation on even more complex orbits. We provide an additional example in Figure 6.

## 5 Conclusions and Perspectives

While agents with behavior-based interactions are relatively easy to implement, it is widely recognized that the underlying mathematical analysis of such models is generally difficult and often even impossible to perform completely. It is therefore quite remarkable that very simple analytical results can be derived for a whole class of dynamics which, due to its simplicity, offers potential for applications. Despite that for

limited number of agents, typically one hundred in our present study, the mean-field approach can only be approximative, we nevertheless emphasize that all our numerical investigations still closely match the theoretical predictions. The resilience of our modeling approach opens several perspectives for implementations on actual agents. Several further research directions are naturally suggested by this contribution, among them:

a) *Extended MCD dynamics to higher dimensional spaces*. The role played here by the Hamiltonian function leading to a canonical motion on the plane can be extended. In particular one may consider, along the lines explained in (Schweitzer, Ebeling and Tilch, 2001), integrable canonical systems exhibiting additional constants of the motions. Using these extra constants of the motion, one will be able to stabilize the swarm motion along orbits in higher dimensions.

b) *Heterogeneity in agents and soft control of swarms.* Instead of focusing on homogeneous agents and by following the work (Han, Li and Guo, 2006), we intend to use the context of MCD to study the possibility to influence (i.e. *soft control*) the behavior by introducing into the society a single "fake" agent (i.e. a *shill*), playing the role of a *leader*, and which can be externally controlled.

c) *Resilience of the modeling.* In Eq. (2), we used the Euclidean norm to define $\mathcal{D}_{k,\rho}(t)$, the instantaneous neighboring agents in Eq. (3). To match specific applications, other type of norms could be used to redefine the interactions.

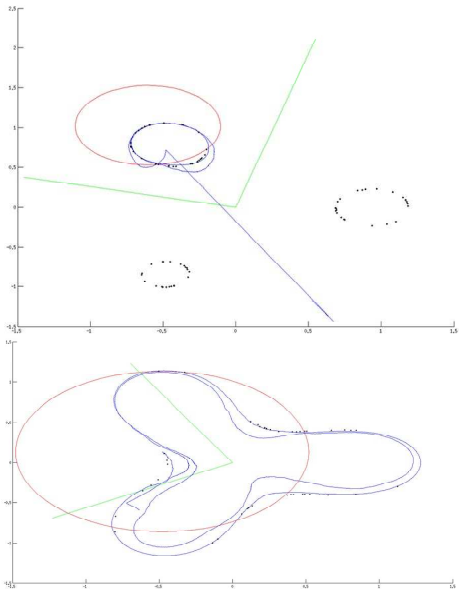

Figure 6: Top: Orbit generated by the $(\frac{2\pi}{3})$-symmetric Hamiltonian function: $\mathcal{H}(x_1,x_2) = \left[(x_1-1)^2+(x_2)^2\right] \cdot \left[(x_1+\frac{1}{2})^2+(x_2-\frac{\sqrt{3}}{2})^2\right]\left[(x_1+\frac{1}{2})^2+(x_2+\frac{\sqrt{3}}{2})^2\right]$. Here we have $N=100$ and the control parameters are set to $M=4$ and $\rho=0.5$.

Bottom: Here, all parameters are identical, except for the interaction range which is $\rho=1$.

## 6 Acknowldgement

This research has been partly supported by the Swiss National Fund for Scientific research and the ESF project *"Exploring the Physics of Small Devices"*.

## References

Cucker, F. and Smale, S. (2007). Emergent behavior in flocks, *IEEE Transactions on Automatic Control* **52**(5).

Frank, T. D. (2005). *Nonlinear Fokker-Planck Equations*, Springer series in Synergetics, Springer: Complexity.

Gazi, V. and Fidan, B. (2007). *Coordination and control of multi-agent dynamic systems: Models and approaches*, Vol. 4433 LNCS of *Lecture Notes in Computer Science (including subseries Lecture Notes in Artificial Intelligence and Lecture Notes in Bioinformatics)*, Springer.

Gazi, V. and Passino, K. M. (2004). A class of attractions/repulsion functions for stable swarm aggregations, *International Journal of Control* **77**(18): 1567–1579.

Han, J., Li, M. and Guo, L. (2006). Soft control on collective behavior of a group of autonomous agents by a shill agent, *Journal of Systems Science and Complexity* **19**(1): 54–62.

Hongler, M.-O. and Ryter, D. M. (1978). Hard mode stationary states generated by fluctuations, *Zeitschrift für Physik B Condensed Matter and Quanta* **31**(3): 333–337.

Hsieh, M. A., Kumar, V. and Chaimowicz, L. (2008). Decentralized controllers for shape generation with robotic swarms, *Robotica* **26**(5): 691–701.

McKean Jr., H. P. (1966). A class of markov processes assocaietd with nonlinear parabolic equations, *Proc. Natl. Acad. Sci USA* **56**(6): 1907–1911.

Reynolds, C. W. (1987). Flocks, herds, and schools: A distributed behavioral model., *Computers (ACM)* **21**(4): 25–34. Cited By (since 1996): 1704.

Schweitzer, F., Ebeling, W. and Tilch, B. (2001). Statistical mechanics of canonical-dissipative systems and applications to swarm dynamics, *Physical Review E - Statistical, Nonlinear, and Soft Matter Physics* **64**(2 I): 211101–211112.

Sepulchre, R., Paley, D. A. and Leonard, N. E. (2008). Stabilization of planar collective motion with limited communication, *IEEE Transactions on Automatic Control* **53**(3): 706–719.

Vicsek, T., Czirk, A., Ben-Jacob, E., Cohen, I. and Shochet, O. (1995). Novel type of phase transition in a system of self-driven particles, *Physical Review Letters* **75**(6): 1226–1229. Cited By (since 1996): 1354.